

## Probability analysis of contact forces in quasi-solid-liquid phase transition of granular shear flow

Ji ShunYing\*

*State Key Laboratory of Structural Analysis for Industrial Equipment, Dalian University of Technology, Dalian 116023, China*

Received July 2, 2012; accepted September 5, 2012; published online January 21, 2013

The quasi-solid-liquid phase transition exists widely in different fields, and attracts more attention due to its instinctive mechanism. The structure of force chains is an important factor to describe the phase transition properties. In this study, the discrete element model (DEM) is adopted to simulate a simple granular shear flow with period boundary condition on micro scale. The quasi-solid-liquid phase transition is obtained under various volume fractions and shear rates. Based on the DEM results, the probability distribution functions of the inter-particle contact force are obtained in different shear flow phases. The normal, tangential and total contact forces have the same distributions. The distribution can be fitted as the exponential function for the liquid-like phase, and as the Weibull function for the solid-like phase. To describe the progressive evolution of the force distribution in phase transition, we use the Weibull function and Corwin-Ngan function, respectively. Both of them can determine the probability distributions in different phases and the Weibull function shows more reasonable results. Finally, the force distributions are discussed to explain the characteristics of the force chain in the phase transition of granular shear flow. The distribution of the contact force is an indicator to determine the flow phase of granular materials. With the discussions on the statistical properties of the force chain, the phase transition of granular matter can be well understood.

**granular materials, quasi-solid-liquid phase transition, force chain, statistical characteristics, simple shear flow**

**PACS number(s):** 45.70.Mg, 47.57.Gc, 04.60.Nc, 81.05.Rm, 45.70.Qj

**Citation:** Ji S Y. Probability analysis of contact forces in quasi-solid-liquid phase transition of granular shear flow. *Sci China-Phys Mech Astron*, 2013, 56: 395–403, doi: 10.1007/s11433-012-4979-z

### 1 Introduction

Phase transition phenomena appear widely in the evolution of ice jamming, dunes flow, landslides and debris flow under natural conditions, and investigations of the phase transition attract more attention for understanding the unique mechanical properties of granular materials [1–5]. The phase transition of granular materials can be divided into two categories. One is the transition between static state (jamming) and dynamic flow state (unjamming) [6–9], and the other is the transition between quasi-static state (solid-like) and rapid flow state (liquid-like) in the shear flow of

granular materials [10–13]. For the first category, most studies focused on the jamming point ( $J$  point) [3,14,15], and the jamming diagram in terms of volume fraction  $\phi$ , shear stress  $\tau$  and granular temperature  $T$  [6–8,16,17]. For the second category, a series of investigations were performed on the mechanical behaviors of dense granular flows under different states to establish the corresponding constitutive models [13,18,19].

The flow state can be determined by the relationship between the average stress and the shear rate in the quasi-solid-liquid phase transition of granular materials [12,13,18,20]. The average stress is proportional to the contact stiffness and independent of the shear rate in the solid-like phase; whereas it is proportional to the square of shear rate and independent of the contact stiffness in the liquid-like phase.

\*Corresponding author (email: jis@dlut.edu.cn)

During the phase transition, this relationship becomes more complex, and is the hot point in establishing the constitutive models of dense granular flows [16,21,22].

The mechanical properties of granular materials at macro scale are related closely to the micro-structure and the interaction between particles at micro scale (i.e., particle scale), which can be described with force chain or force network. The contact force has been determined to describe the characteristics of the phase transition, and the phase diagram was also established [12,13,18]. However, the structure of force chain has an obvious random distribution pattern. For example, the force chain shows strong dynamic characteristics with particles sliding in contact and separation in a shear flow. Consequently, the probability distribution of the contact force,  $P(F)$ , has been examined with numerical simulations or physical experiments [23–28]. With photo-elastic experiments in a biaxial test cell, the probability distribution of the normal and tangential contact force was analyzed under the quasi-static compression and shear conditions [26]. The distributions are affected by the inter-particle friction, the particle shape and hardness [29–32]. However, most of the previous studies worked on the static state or jammed granular system, and the results showed that the probability distribution of the normal force has an exponential tail for forces higher than the average [33–35].

Recently, the force probability distributions were analyzed for dense granular flows [36–38]. Since the force distributions are quite sensitive to the particle location, a tiny change in the inter-particle spacing produces an extremely large change in the force. The measurement of the force distribution has obvious advantages over that of the pair correlation function  $g(r)$ , which is a popular approach to study the micro-structure in granular systems [34]. However, the distributions are quite different for different granular systems. These discrepancies demonstrate the current lack of consensus about the characteristic change in the probability distribution of the contact force. A comprehensive function is still expectant for the quasi-solid-liquid phase transition.

Therefore, we study the quasi-solid-liquid phase transition of a poly-dispersed granular system with soft particles under a simple shear state. The quasi-solid-liquid phase transition is obtained, and the probability distributions of contact forces are analyzed under different shear rates and volume fractions. With the statistical analysis of the micro structure of the force chain, we can learn the mechanical properties of the phase transition of granular shear flows comprehensively.

## 2 Characteristics of the force chain in a granular simple shear flow

### 2.1 Construction of the simple shear flow

We adopt the standard techniques developed for non-equilibrium

molecular dynamics with periodic boundaries to construct a simple shear flow with the discrete element model [12,13]. The computational domain is first filled with a given number of particles to reach a certain volume fraction. The velocity  $V$  is in the  $x$ -direction, with a constant gradient in the  $y$ -direction. When one particle moves out from any direction of the computational domain, it re-enters from the opposite direction to conserve the total granular mass. To obtain a random packing of poly-dispersed granular system at any volume fraction, a face-centered cubic lattice using the maximum particle size to define the lattice points is adopted. After placing the particles, the domain is expanded or compressed to the desired volume according to the prescribed volume fraction. The steady state of the granular shear flow can be obtained after the shearing motion.

In the DEM simulation of granular simple shear flow, the boundaries affect the results if the sample size is too small. Increasing the sample size increases the computational cost sharply. For a simple shear flow of uniform particles, the sample size should be at least  $7D \times 7D \times 7D$ , where  $D$  is the particle diameter [13]. For non-uniform granular materials, boundary effect decreases due to the enhanced disorder from the random distributions of particle size and location. Here, the domain size is chosen to be  $a \times b \times c = (10 \times 10 \times 10) \tilde{D}$  where  $\tilde{D}$  is the mean particle diameter [12]. Here,  $\tilde{D} = 1.0 \times 10^{-2}$  m, and the particle sizes are generated randomly in the range of  $[0.9 \tilde{D}, 1.1 \tilde{D}]$  with a uniform probability function. Figures 1(a) and (b) show the velocity distributions of particles in a steady state at the volume fraction  $\phi = 0.30$  and  $\phi = 0.62$ , respectively.

### 2.2 Force chain structures in granular simple shear flow

The contact force between two spherical particles is simplified as a linear spring and a linear dashpot, that is,  $F_{\text{spring}} = k\delta$  and  $F_{\text{dashpot}} = C\dot{\delta}$ , where  $\delta$  and  $\dot{\delta}$  are the overlap and the relative velocity of the two contacting particles, respectively. These two kinds of forces act in both the normal and the tangential direction of the contact, and the normal and tangential contact forces are written as  $F_n$  and  $F_t$ , respectively. The composition of the two force components is  $F_a = \sqrt{F_n^2 + F_t^2}$ . Their mean values are noted as  $\langle F_n \rangle$ ,  $\langle F_t \rangle$  and  $\langle F_a \rangle$ , with  $\langle \rangle$  meaning the average value. The normal damping coefficient is modeled as  $C_n = \zeta_n \sqrt{(M_A + M_B)K_n}$ , where the dimensionless damping  $\zeta_n$  is defined by the restitution coefficient  $e$  as  $\zeta_n = -\ln e / \sqrt{\pi^2 + \ln^2 e}$ . The tangential stiffness  $K_t = \alpha K_n$ , here  $\alpha = 1.0$ , and the tangential damping force is ignored [12,18]. The tangential force is limited by a friction slider

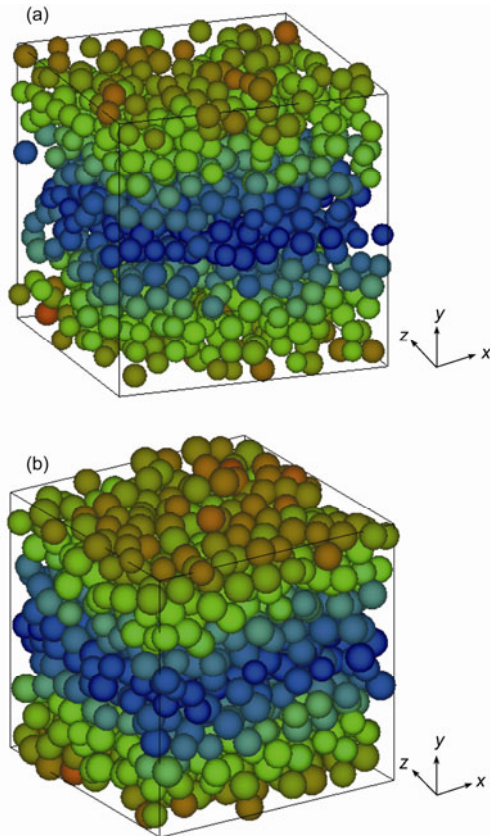


**Figure 1** (Color online) Shear velocity distributions at  $\phi = 0.30$  (a) and  $\phi = 0.62$  (b). Here particles with high velocity are in light color, and those with low velocity are in dark color.

such that the maximum tangential contact force equals  $\mu$  times the normal contact force.

Here, the particle density  $\rho = 1.0 \times 10^3 \text{ kg/m}^3$ , the mean stiffness  $\tilde{K}_n = 1.0 \times 10^7 \text{ N/m}$ , the friction coefficient between particles  $\mu = 0.5$ , and the coefficient of restitution  $e = 0.7$ . To study the shear flow generally, we define a dimensionless shear rate  $B = \dot{\gamma} \sqrt{\rho \tilde{D}^3 / \tilde{K}_n}$ . The volume fraction  $\phi$  and the dimensionless shear rate  $B$  are chosen to be in a wide range of 0.30–0.65 and  $1.0$ – $1.0 \times 10^{-4}$ , respectively, to obtain a comprehensive phase transition from solid-like to liquid-like phase.

Figure 2 plots the force chain distributions at  $B = 1.0 \times 10^{-2}$  and  $\phi = 0.40, 0.50$  and  $0.60$ , respectively. It shows the density and strength of the force chain increase with the increasing volume fraction. The mean contact force  $\langle F_a \rangle$  is 0.13 N, 0.21 N and 1.67 N, respectively.

To investigate the influence of the shear rate, we plot the force chain distributions in Figure 3 when the volume fraction  $\phi = 0.54$  and the dimensionless shear rate  $B = 1.0 \times 10^{-1}, 1.0 \times 10^{-2}$  and  $1.0 \times 10^{-3}$ , respectively. The strength and density of force chain increase with the decreasing shear rate  $B$ . Therefore, the force chain density and strength are quite different under various shear rates and volume fractions.

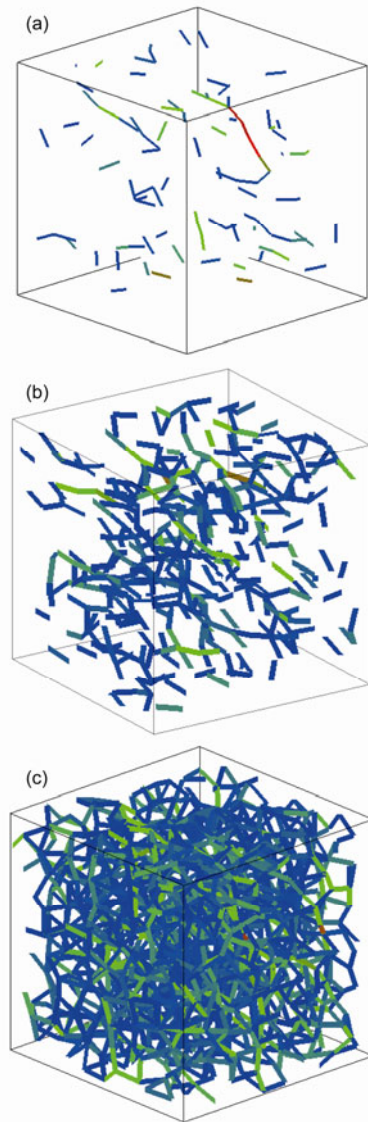


**Figure 2** (Color online) Force chain distributions at various volume fractions when the dimensionless shear rate  $B = 1.0 \times 10^{-2}$ . (a)  $\phi = 0.40$ ; (b)  $\phi = 0.50$ ; (c)  $\phi = 0.60$ .

### 2.3 Quasi-solid-liquid phase transition in the granular shear flow

Figure 4 plots the contact force  $\langle F_a \rangle$  with different volume fractions in the range of 0.30–0.65 and dimensionless shear rates in the range of  $1.0$ – $1.0 \times 10^{-4}$ . It shows  $\langle F_a \rangle$  is independent of the shear rate  $B$  at higher volume fraction  $\phi$ , and increases with  $B$  linearly in the logarithmic coordinates at lower volume fraction. This distribution is similar to that of the average stress, which was adopted to analyze the phase transition of granular shear flow [12,13]. The granular material exhibits solid-like behavior when the stress (or contact force) is independent of the shear rate, otherwise with liquid-like behavior. Figure 5 plots the phase diagram for the quasi-solid-liquid transition, by considering the average

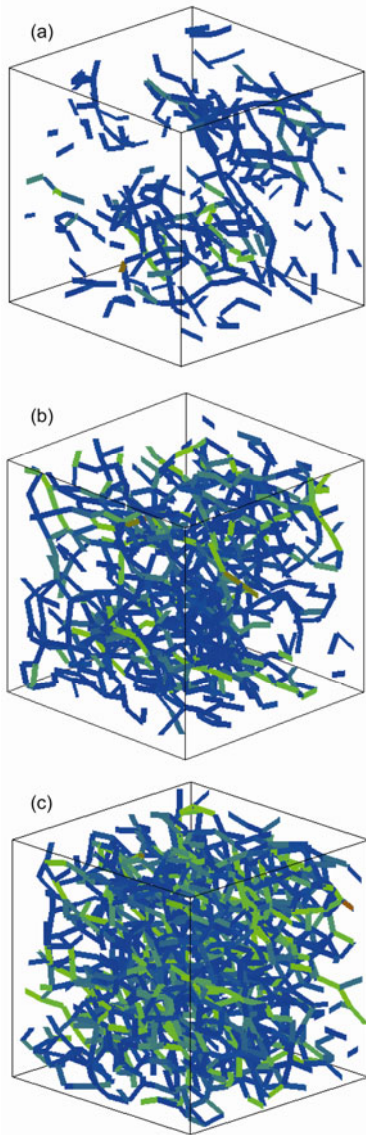


**Figure 3** (Color online) Force chain distributions at various shear rates when the volume fraction  $\phi=0.54$ . (a)  $B=1.0\times 10^{-1}$ ; (b)  $B=1.0\times 10^{-2}$ ; (c)  $B=1.0\times 10^{-3}$ .

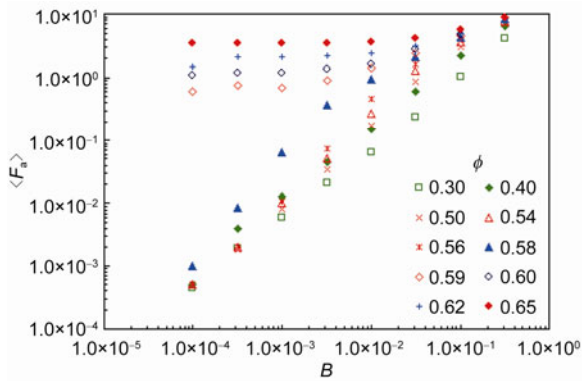


**Figure 4** (Color online) Distributions of the contact force in the quasi-solid-liquid phase transition of granular shear flow.

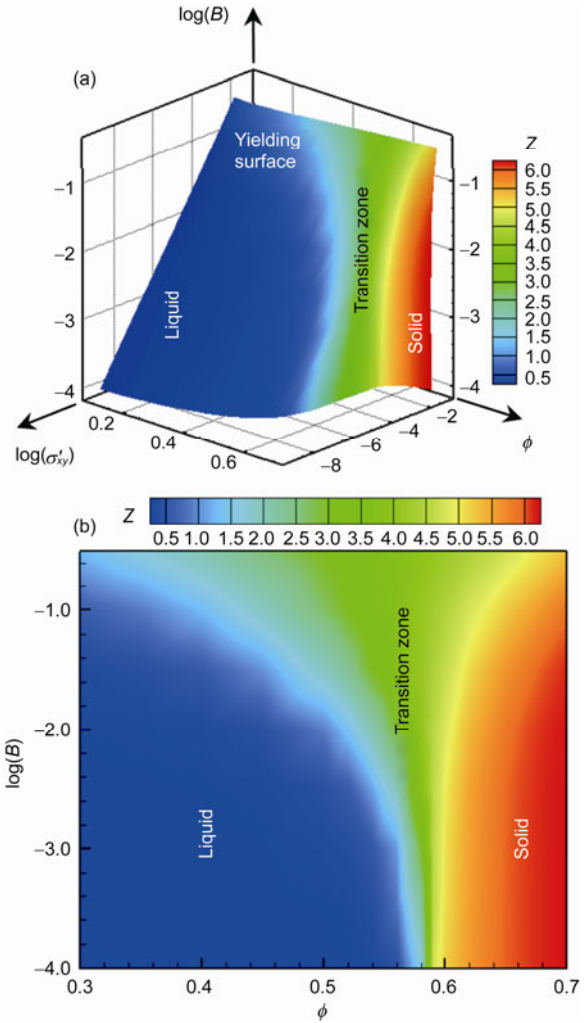


**Figure 5** Phase diagram of the quasi-solid-liquid phase transition of granular shear flow. (a) Phase diagram in 3D; (b) phase diagram in 2D.

dimensionless stress  $\sigma'_{ij} = \sigma_{ij} \tilde{D} / \tilde{K}_n$  ( $i, j = 1, 2, 3$ ) [39]. In this phase diagram, the coordination number is given to show the evolution of phase transition distinctly. This diagram gives a global view of the quasi-solid-liquid phase transition under various shear rates and volume fractions.

### 3 Probability analysis of the contact force in phase transition

#### 3.1 Probability distribution of contact forces in the solid-like and liquid-like phase

To compare the probability distributions of forces in normal and tangential directions, we select two cases in the phase diagram. One is in the liquid-like phase with  $\phi = 0.50$  and  $B=1.0\times 10^{-3}$ , and the other is in the solid-like phase with  $\phi = 0.60$  and  $B=1.0\times 10^{-4}$ . Here, the normalized contact force  $f = F/\langle F \rangle$  is introduced to analyze the probability of the force

chain strength. The normalized inter-particle normal, tangential and total contact forces are written as  $f_n$ ,  $f_t$  and  $f_a$ , respectively, with variable  $F$  representing corresponding  $F_n$ ,  $F_t$ , or  $F_a$ . Figures 6 and 7 plot the probability distributions of contact forces in the liquid-like and solid-like phase, respectively. In the same phase, all the contact forces have similar probability distributions, while the shape of the probability function is quite different for different phases.

The probability distribution function of the normalized total force in the liquid-like phase (as shown in Figure 6), appears as an exponential distribution, and can be written as:

$$P(f_a) = Ae^{-Af_a}, \tag{1}$$

where  $f_a$  is the normalized total contact force. The parameter  $A$  is determined to be 1.080.

The probability distribution function of the normalized total force in the solid-like phase (as shown in Figure 7), can be fitted by the Weibull probability distribution function as:

$$P(f_a) = \frac{k}{\lambda} \left(\frac{f_a}{\lambda}\right)^{k-1} e^{-\left(\frac{f_a}{\lambda}\right)^k}, \tag{2}$$

where the parameters  $k$  and  $\lambda$  are determined as  $k=1.286$  and  $\lambda=1.107$ , respectively.

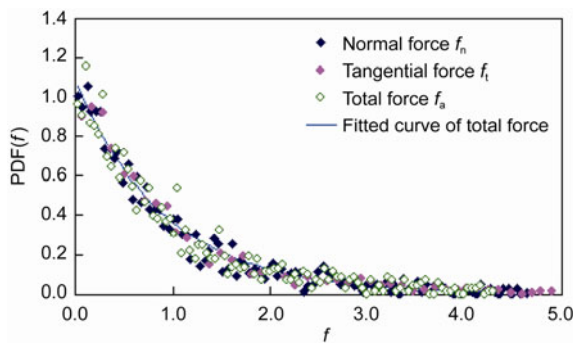


**Figure 6** (Color online) Probability distributions of contact forces in the liquid-like phase ( $\phi=0.50$  and  $B=1.0\times 10^{-3}$ ).

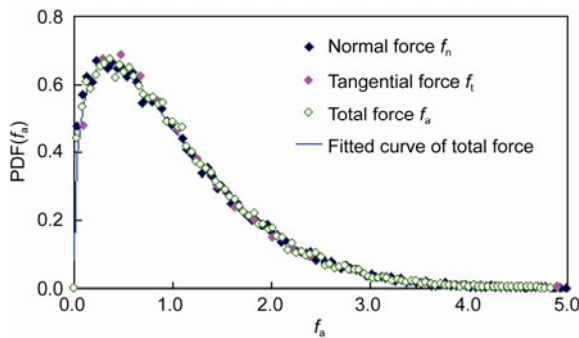


**Figure 7** (Color online) Probability distributions of contact forces in the solid-like phase ( $\phi=0.60$  and  $B=1.0\times 10^{-4}$ ).

Comparing eqs. (1) and (2), we find the exponential distribution is a special type of Weibull distribution. In fact, eq. (1) can also be written in the form of eq. (2) with the parameter  $k=1.0$  and  $\lambda=A^{-1}=0.926$ , respectively. In both cases, the probability distribution function decays exponentially for large force. These characteristics have been verified in many experimental results and numerical simulations [23,26,33–35].

### 3.2 Evolution of contact force distributions during phase transition

By keeping the dimensionless shear rate as a constant of  $B=1.0\times 10^{-2}$ , the granular system transforms from the liquid-like phase to the solid-like phase when the volume fraction  $\phi$  is increased from 0.30 to 0.65. Figure 8(a) plots the probability distributions at the volume fractions of 0.40, 0.50, 0.56 and 0.60, respectively. The Weibull probability function of eq. (2) is adopted to fit the normalized contact forces. The fitting curves are also plotted in Figure 8(a), and the probability parameters are listed in Table 1. The fitted curves show that the Weibull function describes effectively the probability distribution from the solid-like phase to the liquid-like phase. For the solid-like phase, such as  $B=1.0\times 10^{-2}$ ,  $\phi=0.60$ ,  $P(f_a)$  has a peak at  $f_a=0.60$ . For large contact force,  $P(f_a)$  approaches zero when  $f_a > 4.0$ ; For small contact force,  $P(f_a)$  is about 0.35 when  $f_a \rightarrow 0.0$ . For the liquid-like phase, such as  $B=1.0\times 10^{-2}$ ,  $\phi=0.40$ ,  $P(f_a)$  has the maximum value when  $f_a \rightarrow 0.0$ , and then decreases exponentially with the increasing contact force. In this situation, the parameter  $k=1.015$ , which is close to 1.0. It is a perfect exponential distribution when  $k=1.0$ . In other words,  $P(f_a)$  is an exponential function in the liquid-like phase.

Similarly, by keeping the volume fraction as a constant of  $\phi=0.56$ , the granular system transforms from the solid-like phase to the liquid-like phase. Figure 8(b) shows the corresponding probability distribution of the normalized contact forces with  $B=1.0\times 10^{-1}$ ,  $1.0\times 10^{-2}$ ,  $1.0\times 10^{-3}$  and  $1.0\times 10^{-4}$ , respectively. The evolution of the contact force distributions from the solid-like phase to the liquid-like phase is quite similar to that in Figure 8(a). Still using the Weibull distribution function, the parameters are determined in different phases as listed in Table 1. In this situation, the parameter  $k=0.993$ , which is also close to 1.0, in the liquid-like phase with  $B=1.0\times 10^{-2}$  and  $\phi=0.56$ . Therefore, the distribution can also be matched with the exponential function.

From Figure 8, we can find the Weibull function can describe the contact force distributions in both solid-like and liquid-like phases. During the phase transition by changing either the shear rate or the volume fraction, the force chain probability distributions have similar trends. Especially the parameter  $k$  decreases from around 1.40 to 1.0 in the phase transition from the solid-like to the liquid-like phases. In the

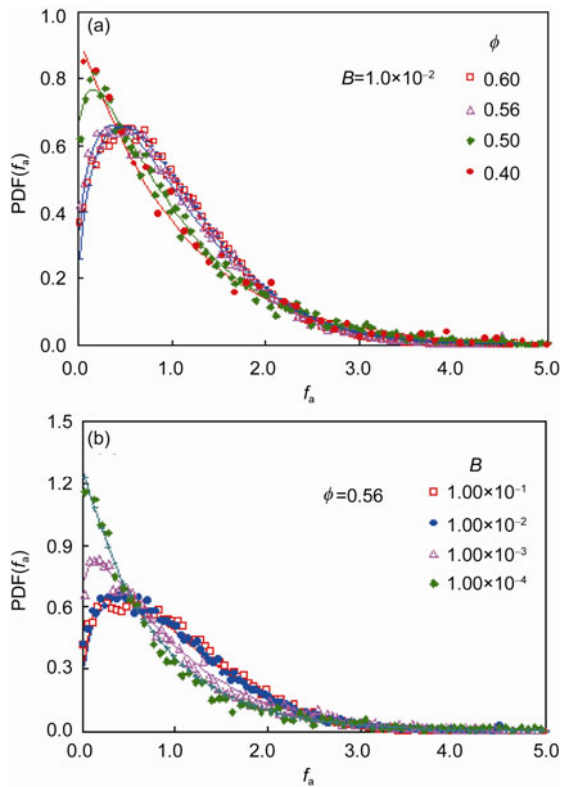


**Figure 8** (Color online) Probability distribution of the normalized contact force under different phases of granular shear flow.

**Table 1** Distribution parameters of the contact force with the Weibull function

$\phi$	$B = 1.0 \times 10^{-2}$		$\phi = 0.56$		
	$k$	$\lambda$	$B$	$K$	$\lambda$
0.60	1.406	1.124	$1.0 \times 10^{-1}$	1.342	1.149
0.56	1.315	1.113	$1.0 \times 10^{-2}$	1.315	1.114
0.50	1.128	1.025	$1.0 \times 10^{-3}$	1.122	0.972
0.40	1.015	1.040	$1.0 \times 10^{-4}$	0.993	0.788

liquid-like phase, the probability function also transforms from the Weibull function to the exponential function via  $k \rightarrow 1.0$ . In the physical experiment of Mueth et al. [33], the probability of a bead having a certain force decays exponentially as  $P(f) \propto e^{-\beta f}$ , with  $\beta = 1.5 \pm 0.1$  for the forces greater than the mean  $f=1$ . Moreover, the exponent in the exponential part of the distribution can be 1.8 [40].

#### 4 Discussions on probability distributions of the contact forces in the phase transition

The probability distribution of the contact force is an effective approach to distinguish the micro-structures of force chains in different phases, since the forces are sensitive to minute variations in particle positions. The distribution of

the contact force can serve as a micro-scope to observe the correlation in the positions of the nearest neighbors. In the following, we discuss the phase transition mechanism indicated in the inter-particle contact force distributions.

##### 4.1 Distribution of contact forces in solid-like phase

In the solid-like phase, also called jamming state, the distribution functions of the contact forces were determined with physical experiments and numerical simulations. For the frictional granular system, the probability function  $P(f)$  decays exponentially above the average force, and has a small peak at force magnitude below  $f$ . The characteristic shape of  $P(f)$  has become a signature of a jammed granular system [9,34,35]. From the photo-elastic experiment of the static granular shear system performed by Majmudar et al. (2005), the normal force in the solid-like phase has the similar probability distribution as presented in this work, but the distributions of the tangential force are quite different. The peak in the probability distribution disappears under large shear strain [28]. For the granular system compressed in a cylindrical container, the distributions of contact forces are affected by the boundary and stress level [25]. Van Hecke discussed the probability distribution of the contact force in the static state with the photo-elastic results, and also compared with others results. He found a change in the 'tail' of the distributions (characterizing the particles carrying the largest forces). Jammed granular systems produce tails with an exponential fall-off, whereas yielded systems produce much steeper tails. Thus, flowing grains can avoid large forces more effectively than those that are jammed [41].

With carbon paper and elasticphone grains, the normal force distributions on the box bottom boundary were determined. An exponential function was adopted to fit the force distribution as [23]:

$$P(f) = Ce^{-Af}, \quad (3)$$

where parameters were determined as  $A=0.64 \text{ N}^{-1}$ ,  $C=988$  for the total region, and  $A=1.02 \text{ N}^{-1}$ ,  $C=736$  for the inner region.

With the measurements of the normal forces distributed in the static granular system under uniaxial compression, a probability distribution function was developed as [33]:

$$P(f) = a(1 - be^{-f^2})e^{-\beta f}, \quad (4)$$

where  $a = 3.0$ ,  $b = 0.75$  and  $\beta = 1.5$ , respectively. Their results also show the exponential tail as  $P(f) \propto e^{-\beta f}$  at large  $f$ , a flattening out of the distribution near  $f \sim 1$ , and a slight increase in  $P(f)$  as  $f$  decreases towards zero.

For the static granular system, the distribution function  $P(f)$  normally has the form as [40]:

$$P(f) \propto \begin{cases} f^\alpha, & \text{if } f < 1, \\ e^{-\beta f}, & \text{if } f > 1. \end{cases} \quad (5)$$

Müller et al. [42] discussed the distribution forms in detail. From the functions above, we can find large contact forces exhibit exponential decay, such that the equation forms can be different.

#### 4.2 Distribution of contact forces in liquid-like phase

For the contact force distribution in a granular flow, some attempts were made to demonstrate the mechanical properties of granular system on micro scale. Longhi et al. [36] measured the normal component of impulses (impact force) in a granular hopper flow and found the large forces have the exponential tails at different flow rates, but the distributions of small forces change with the flow rate. At slower flow rates,  $P(f)$  tends to move upwards rather than bends down, and forms a peak.

For the sake of describing the large contact force distributions in a shear cell under different shear rates, a complex distribution function was established considering the elastic potential in the particle deformation with the Hertzian contact force model as [34]:

$$P(f) = a \left[ 1 + f^{2/3} \frac{\langle \Delta \rangle}{d} \right]^2 \frac{1}{f^{1/3}} \exp\left(-\frac{\zeta}{\zeta_0} f^{5/3}\right), \quad (6)$$

where  $a$  is a normalized constant,  $\langle \Delta \rangle$  is the average deformation of a particle,  $d$  is the particle diameter, and the parameter  $\zeta = 1/(k_B T)$ . Here  $T$  is the granular temperature, and  $k_B$  is the Boltzmann's constant.  $1/\zeta_0$  is a temperature scale set by the average force per bead and the bead elastic modulus. For small forces, the distribution function can be written as  $P(f) \propto f^{-1/3}$ . With this equation, the contact force distributions match the experimental data well. Since the granular temperature  $T$ , which can be thought of as an index of shear rate in a granular system, is considered in eq. (6), the distribution of contact forces can be fitted in both solid-like and liquid-like phases [34].

Recently, eq. (6) was applied well in the normal and tangential contact force distributions in 2-D annular shear granular systems simulated with the linear contact force model under different shear rates and volume fractions [43,44]. Chan and Ngan [45] discussed the rationality of eq. (6) based on the contact force model between particles, and then worked out a simplified form to analyze their experimental data as:

$$P(f) = a \exp(-k(f^{5/3} - bf^{2/3})). \quad (7)$$

In their experiments, the polystyrene spheres were packed in an acrylic tank. With random and regular HCP (Hexagonal-close-packed) packing patterns, different force

distributions were obtained. The value of  $k$  is in the range of 0.2–0.4 for random packing, while it is in the range of 2.0–3.0 for the HCP packing. Under high pressure with HCP packing, the value of  $k$  can increase to 4.0 [46]. The indication of  $k$  value means the shapes of distribution. Small value of  $k$  means the narrow shape of the distribution function and rapid decay of the contact force. Moreover, the parameter  $a$  means the probability density at  $f=0$ . Here, we call eq. (7) Corwin-Ngan function for convenient discussion of the distribution characteristics below.

In this work, the probability distributions of the normalized contact force  $f_a$  are analyzed with eq. (7) in different phases. With constant dimensionless shear rate  $B=1.0 \times 10^{-2}$ , the distributions are plotted in Figure 9(a) when the volume fraction  $\phi = 0.40, 0.50, 0.56$  and  $0.60$ , respectively. With the increasing volume fraction, the granular system shows phase transition from the liquid-like to the solid-like. The parameter  $k$  increases from 0.303 at  $\phi = 0.40$ –0.877 at  $\phi = 0.60$ . Moreover, if the volume fraction is kept as a constant of  $\phi = 0.56$ , and the shear rate  $B$  is increased from  $1.0 \times 10^{-4}$  to  $1.0 \times 10^{-1}$ , the phase transition from the solid-like to the liquid-like can also be obtained. The distributions of the contact force are plotted in Figure 9(b), and the parameters are listed in Table 2. We can also find the similar evolution of parameter  $k$ . From the fitted curves in different phases, as shown in Figure 9, we can conclude that eq. (7) can also

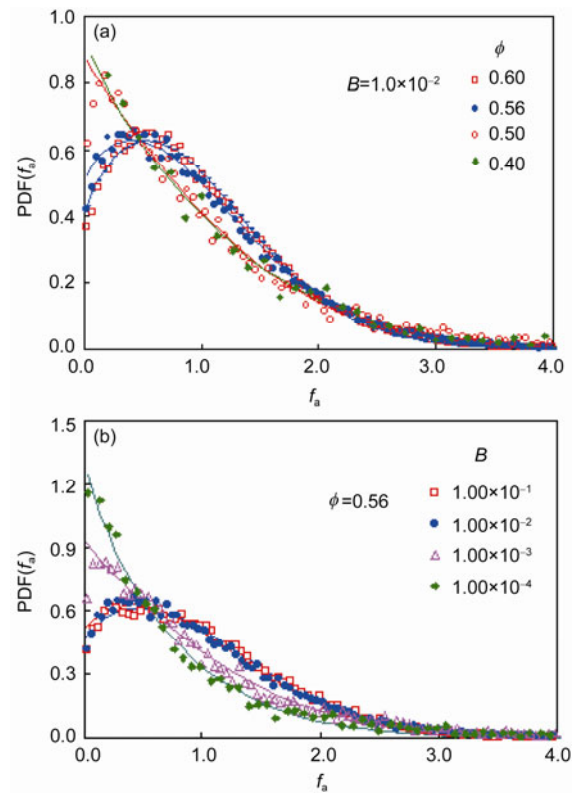


Figure 9 (Color online) Probability distribution of the contact force under different phases of a granular shear flow.

**Table 2** Fitted parameters for the distribution of contact force

$\phi$	$B=1.0\times 10^{-2}$			$\phi=0.56$			
	$a$	$k$	$b$	$B$	$a$	$k$	$b$
0.60	0.391	0.877	1.354	$1.0\times 10^{-1}$	0.447	0.725	1.185
0.56	0.492	0.723	1.023	$1.0\times 10^{-2}$	0.492	0.723	1.023
0.50	0.899	0.383	-1.025	$1.0\times 10^{-3}$	0.954	0.431	-0.973
0.40	0.967	0.303	-1.889	$1.0\times 10^{-4}$	1.378	0.428	-2.285

well describe the probability distributions in different phases. Further, Figure 9 and Table 2 show that the value of  $a$  increases during the transition from the solid-like to the liquid-like phase, and the value of  $b$  decreases during this transition.

With eqs. (2) and (7), the probability distributions during phase transition can be simulated efficiently both by the Weibull function and the Corwin-Ngan function, and the Weibull function can match the data better as seen in Figures 8 and 9. But the three parameters in the Corwin-Ngan function, i.e.,  $k$ ,  $a$  and  $b$  in eq. (7), have obvious meanings. In fact, the variable  $k/\lambda$  in eq. (2) is equivalent to the variable  $a$  in eq. (7) when  $f_a \rightarrow 0.0$ .

### 4.3 Indication of the contact force distributions in phase transition

The probability distribution of the contact force indicates the interaction between particles, and has close relationship with the behaviors of granular flow. Based on the probability analysis above, the distribution shapes are quite different in the solid-like and the liquid-like phases, and have a progressive evolution between the two phases.

In the liquid-like phase, the granular system flows rapidly under low volume fraction. Most of the interactions between particles are in binary contact manner, and are dominated by the shear velocity. In this way, the particle contacts are quite weak accompanied with small elastic deformation between particles. Meanwhile, some large contact forces can also occur stochastically. The particles flow with a certain velocity under a random fluctuation. The fluctuations of the particle velocity have been observed in the granular flow systems, such as in shear cell test [47]. Therefore, the small contact force has high probability distribution in the liquid-like phase. With the increasing contact force, the probability decreases exponentially.

In the solid-like phase, the particles have large elastic deformation with low velocity. The contact forces among particles are dominated by the deformation instead of the particle velocity. Since the stochastic distribution of the force chain is in the spatial domain, the distribution curve of the contact force has a peak at about  $0.50f_a$ , and decays exponentially with the increasing contact force. Moreover, the probability of small contact force can also occur. The distribution of the contact force was also observed in the jamming state of granular systems [9,24,26,48].

From Figures 8 and 9, we can find the progressive evolution of the contact force distributions from the solid-like to the liquid-like phase. The difference is the location of the distribution peak. The peak is located at the lowest force for the liquid-like phase, and located at  $0.50f_a$  for the solid-like phase. For the lowest force, the probability density  $P(f_a \rightarrow 0.0)$  is about 0.40 in the solid-like phase, and is about 1.20 in the liquid-like phase. During the transition from the solid-like phase to the liquid like phase, the probability density of small contact force increases continuously. This indicates the granular system is more liquid-like, and more small contact forces appear. In this situation, the granular system is more instable. Moreover, from the trails of the contact force distribution (as shown in Figures 8 and 9), we can find the force distribution in a liquid-like system decays more rapidly than that in a solid-like system. The distributions in various phases approach zero when  $f_a > 4.0$ . From the shapes of the contact force distribution, the phase of the granular flow can be indentified.

## 5 Conclusions

During the quasi-solid-liquid phase transition of a granular shear flow, the mechanical behaviors of the granular system at macro scale are dominated by the inter-particle contact forces at micro scale. The probability analysis on the contact forces can help understand the internal mechanism of phase transition of the granular system. In this study, the discrete element model is adopted to simulate the simple granular shear flow. The quasi-solid-liquid phase transition is obtained under various volume fractions and shear rates. Based on the phase diagram of the granular shear system, the normalized contact force distributions are analyzed in different phases. The normal, tangential and total forces have the same probability distribution. Here, the normalized total contact force is analyzed. The Weibull function fits the simulated results well in the solid-like phase, while the exponential function matches the data in the liquid-like phase. To determine the progressive evolution of the force distribution during phase transition, we use the Weibull function to fit the contact force in various phases. Meanwhile, the Corwin-Ngan function is adopted to describe the probability distribution of the contact force during the phase transition. Both of them match the contact force distribution effectively. The indication of the force distribution on force chains is

discussed. With the determination of the force distribution during the phase transition, the mechanism of granular behaviors can be understood well under different flow phases.

*This work was supported by the National Basic Research Program of China (Grant No. 2010CB731502) and the Fundamental Research Funds for the Central Universities (Grant No. DUT12YQ02).*

- 1 Jaeger H M, Nagel S R. Physics of the granular state. *Science*, 1992, 255: 1523–1531
- 2 GDR M. On dense granular flows. *Eur Phys J E*, 2004, 14: 341–365
- 3 Song C, Wang P, Makse H A. A phase diagram for jammed granular matter. *Nature*, 2008, 453: 629–632
- 4 Lu K, Brodsky E E, Kavehpour H P. A thermodynamic unification of jamming. *Nat Phys*, 2008, 4: 404–407
- 5 Reichhardt C J O, Reichhardt C. Fluctuations, jamming, and yielding for a driven probe particle in disordered disk assemblies. *Phys Rev E*, 2010, 82: 051306
- 6 Liu A J, Nagel S R. Jamming is not just cool any more. *Nature*, 1998, 396: 21–22
- 7 O'Hern C S, Lander S A, Liu A J, et al. Random packings of frictionless particles. *Phys Rev Lett*, 2002, 88(7): 075507
- 8 Cheng X. Experimental study of the jamming transition at zero temperature. *Phys Rev E*, 2010, 81: 031301
- 9 Wang P, Song C, Briscoe C, et al. From force distribution to average coordination number in frictional granular matter. *Phys A*, 2010, 389: 3972–3977
- 10 Biroli G. Jamming—A new kind of phase transition? *Nat Phys*, 2007, 3: 222–223
- 11 Candelier R, Dauchot O. Journey of an intruder through the fluidization and jamming transitions of a dense granular media. *Phys Rev E*, 2010, 81: 011304
- 12 Ji S, Shen H. Internal parameters and regime map for soft poly-dispersed granular materials. *J Rheol*, 2008, 52(1): 87–103
- 13 Campbell C S. Granular shear flows at the elastic limit. *J Fluid Mech*, 2002, 465: 261–291
- 14 Somfai E, van Hecke M, Ellenbroek W G, et al. Critical and noncritical jamming of frictional grains. *Phys Rev E*, 2007, 75: 020301
- 15 Berthier L, Witten T A. Glass transition of dense fluids of hard and compressible spheres. *Phys Rev E*, 2009, 80: 021502
- 16 Lois G, Lemaitre A, Carlson J. Numerical tests of constitutive laws for dense granular flows. *Phys Rev E*, 2005, 72: 051303
- 17 Zhang Z, Xu N, Chen D T N, et al. Thermal vestige of the zero-temperature jamming transition. *Nature*, 2009, 459: 230–233
- 18 Babic M, Shen H H, Shen H T. The stress tensor in granular shear flows of uniform, deformable disks at high solids concentrations. *J Fluid Mech*, 1990, 219: 81–118
- 19 Yan Y, Ji S. Energy conservation in a granular shear flow and its quasi-solid-liquid transition. *Part Sci Technol*, 2009, 27(2): 126–138
- 20 Shen H H, Sankaran B. Internal length and time scales in a simple shear granular flow. *Phys Rev E*, 2004, 70: 051308
- 21 Elaskar S A, Godoy L A, Gray D D, et al. A viscoplastic approach to model the flow of granular solids. *Int J Solids Struct*, 2000, 37(15): 2185–2214
- 22 Jop P, Forterre Y, Pouliquen O. A constitutive law for dense granular flows. *Nature*, 2006, 441(8): 727–730
- 23 Liu C H, Nagel S R, Schecter D A, et al. Force fluctuations in bead packs. *Science*, 1995, 269: 513–515
- 24 Radjai F, Jean M, Moreau J J, et al. Force distributions in dense two-dimensional granular systems. *Phys Rev Lett*, 1996, 77: 274–277
- 25 Liu L, Zhang L, Liao S. Structural signature and contact force distributions in the simulated three-dimensional sphere packs subjected to uniaxial compression. *Sci China-Phys Mech Astron*, 2010, 53: 892–904
- 26 Majmudar T S, Behringer R P. Contact force measurements and stress-induced anisotropy in granular materials. *Nature*, 2005, 435: 1079–1082
- 27 Zhou J, Long S, Wang Q, et al. Measurement of forces inside a three-dimensional pile of frictionless droplets. *Science*, 2006, 312: 1631–1633
- 28 Kruyt N P, Rothenburg L. Probability density functions of contact forces for cohesionless frictional granular materials. *Int J Solids Struct*, 2002, 39: 571–583
- 29 Silbert L E, Grest G S, Landry J W. Statistics of the contact network in frictional and frictionless granular packings. *Phys Rev E*, 2001, 66: 061303
- 30 Blair D L, Mueggenburg N W, Marshall A H, et al. Force distributions in three-dimensional granular assemblies: Effects of packing order and interparticle friction. *Phys Rev E*, 2001, 63: 041304
- 31 Erikson J M, Mueggenburg N W, Jaeger H M, et al. Force distributions in three-dimensional compressible granular packs. *Chem Phys*, 2010, 375: 600–605
- 32 Azéma E, Radjai F, Saussine G. Quasistatic rheology, force transmission and fabric properties of a packing of irregular polyhedral particles. *Mech Mater*, 2009, 41: 729–741
- 33 Mueth D M, Jaeger H M, Nagel S R. Force distribution in a granular medium. *Phys Rev E*, 1998, 57: 3164–3169
- 34 Corwin E I, Jaeger H M, Nagel S R. Structural signature of jamming in granular media. *Nature*, 2005, 435: 1075–1078
- 35 O'Hern C S, Langer S A, Liu A J, et al. Force distributions near jamming and glass transitions. *Phys Rev Lett*, 2001, 86: 111–114
- 36 Longhi E, Easwar N, Menon N. Large force fluctuations in a flowing granular medium. *Phys Rev Lett*, 2002, 89: 045501
- 37 Landry J W, Grest G S, Plimpton S J. Forces in granular hopper flow. *Bull Am Phys Soc*, 2003, 48: 153
- 38 Ferguson A, Fisher B, Chakraborty B. Impulse distributions in dense granular flows: Signatures of large-scale spatial structures. *Eur Phys Lett*, 2004, 66: 277–283
- 39 Ji S, Sun Q, Yan Y. Characteristics in quasi-solid-liquid phase transition of granular shear flow and its phase diagram (in Chinese). *Sci Sin-Phys Mech Astron*, 2011, 41: 1112–1125
- 40 Lovoll G, Maloy K J, Flekkoy E G. Force measurements on static granular materials. *Phys Rev E*, 1999, 60(5): 5872–5878
- 41 van Hecke M. A tale of tails. *Nature*, 2005, 435: 1041–1042
- 42 Müller M K, Luding S, Pöschel T. Force statistics and correlations in dense granular packings. *Chem Phys*, 2010, 375: 600–605
- 43 Wang D, Zhou Y. Particle dynamics in dense shear granular flow. *Acta Mech Sin*, 2010, 26: 91–100
- 44 Wang D, Zhou Y. Statistics of contact force network in dense granular matter. *Particuology*, 2010, 8: 133–140
- 45 Chan S H, Ngan A H W. Statistical distribution of contact forces in packings of deformable spheres. *Mech Mater*, 2005, 37: 493–506
- 46 Ngan A H W. On distribution of contact forces in random granular packings. *Phys A*, 2004, 339: 207–227
- 47 Hsiau S S, Yuh-Min S Y M. Effect of solid fraction on fluctuations and self-diffusion of sheared granular flows. *Chem Eng Sci*, 2000, 55: 1969–1979
- 48 Eerd A R T, Ellenbroek W G, Hecke M V, et al. The tail of the contact force distribution in static granular materials. *Phys Rev E*, 2007, 75: 060302